· Article · Advances in Polar Science
doi: 10.13679/j.advps.2020.0015 September 2020 Vol. 31 No. 3: 192-204

Spatial variation in grain-size population of surface sediments from northern Bering Sea and western Arctic Ocean: implications for provenance and depositional mechanisms

WANG Weiguo[1*], YANG Jichao[2], ZHAO Mengwei[3], DONG Linsen[4], JIANG Min[1] & HUANG Erhui[1]

[1] Third Institute of Oceanography, Ministry of Natural Resources (MNR), Xiamen 361005, China;
[2] National Deep Sea Center, Ministry of Natural Resources (MNR), Qingdao 266237, China;
[3] Pilot National Laboratory for Marine Science and Technology, Qingdao 266237, China;
[4] First Institute of Oceanography, Ministry of Natural Resources (MNR), Qingdao 266061, China

Received 25 May 2020; accepted 30 July 2020; published online 20 September 2020

Abstract In general, sediments in nature comprise populations of various diameters. Accurate information regarding the sources and depositional mechanisms of the populations can be obtained through their temporal and spatial comparisons. In this study, the grain size distribution of surface sediments from the Bering Sea and western Arctic Ocean were fitted and partitioned into populations using a log-normal distribution function. The spatial variations in the populations indicate differences in their sources and deposition mechanisms. The sediments on most of the Bering Sea Shelf originated from the Yukon River, and were transported westward by waves and currents. However, the presence of a coarser population outside Anadyr Bay was the result of Anadyr River transport. Additionally, a northward transport trend of fine suspended particles was observed on the west side of the Bering Sea Shelf. The sediments in Hope Valley in the south Chukchi Sea also originated from the Yukon River. The coarser population on the central Chukchi Sea Shelf originated from coast of Alaska to the east, not the Yukon River, and was transported by sea ice and bottom brine water. The populations of sediments from the Chukchi Basin and the base of the Chukchi Sea Slope are the result of sea ice and eddy action. Surface sediments from the western high Arctic Ocean predominantly comprised five populations, and two unique populations with mode diameters of 50–90 μm and 200–400 μm, respectively, were ubiquitous in the glacial and interglacial sediments. It was difficult to distinguish whether these two populations originated from sea ice or icebergs. Therefore, caution should be exercised when using either the > 63 μm or > 250 μm fractions in sediments as a proxy index for iceberg and ice sheet variation in the high Arctic Ocean.

Keywords **Bering Sea, western Arctic Ocean, surface sediments, grain-size population, provenance, depositional mechanisms**

Citation: Wang W G, Yang J C, Zhao M W, et al. Spatial variation in grain-size population of surface sediments from northern Bering Sea and western Arctic Ocean: implications for provenance and depositional mechanisms. Adv Polar Sci, 2020, 31(3): 192-204, doi: 10.13679/j.advps.2020.0015

1 Introduction

Grain size provides information on the provenance, transportation, and depositional environments of sediments. In recent decades, sedimentologists have been mining sedimentary information using grain size distribution (GSD). The grain size parameters, such as mean, sorting, skewness, and kurtosis, obtained from the GSDs of bulk samples have been widely applied in distinguishing depositional

* Corresponding author, ORCID: 0000-0003-0328-8516, E-mail: wangweiguo@tio.org.cn

environments and sediment trend analysis (Folk and Ward, 1957; McManus, 1988; Gao and Collins, 1992; Le Roux and Rojas, 2007; Poizot et al., 2008). However, most GSDs of hydraulic sediments are bi-modal or polymodal, which are formed from various combinations of unimodal populations. Each unimodal population in a polymodal GSD follows a type of natural distribution, representing different transport or depositional processes (Middleton, 1976; Ashley, 1978). Therefore, these aforementioned grain size parameters of bulk samples used as proxy indexes of sedimentary environments may not accurately reflect the sedimentary dynamics or sources (Sun et al., 2002; Weltje and Prins, 2003).

To extract genesis information, partitioning GSDs into populations in bulk samples and spatial comparisons of such populations makes sense. To extract sedimentary information from a polymodal GSD, the methods that are commonly adopted include end-member modeling analysis (Prins et al., 2000; Weltje and Prins, 2007), sensitive grain-size component extraction based on the standard deviation (Fan et al., 2011; Zhou et al., 2014), and Weibull or log-normal distribution function fitting (Sun et al., 2002; Qin et al., 2005). These methods have been applied in studies of eolian, lake, and marine sediments (Sun et al., 2002; Nagashima et al., 2012; Xiao et al., 2012; Park et al., 2014a).

The sediments in the Bering Sea and western Arctic Ocean have various sources and complex depositional processes (Naidu et al., 1982; Darby, 2003; Viscosi-Shirley et al., 2003; Asahara et al., 2012; Nagashima et al., 2012; Nwaodua et al., 2014; Park et al., 2014b; Watanabe et al., 2014). The results regarding the sediment sources in this region obtained by previous researchers using different methods are controversial. This may be because the studies used different sediment grain-size fractions, such as clay, silty, or sandy fractions, or even bulk samples, as material for mineral, ice-rafted debris (IRD), and geochemical study. Determining the sources and transport trends of various populations of sediments in the study area is of great importance for reconstructing the paleoceanographic evolution of the Arctic Ocean as well as for predicting the fate of pollutants.

The most defining feature of sediments in the high Arctic Ocean that sets them apart from those in other oceans is that they contain IRD, which can be transported both by icebergs (derived from land-based ice) and by sea ice. It is critical to differentiate sea ice from glacial (land-based) ice as climate feedback mechanisms and global impacts differ between these systems (Stickley et al., 2009). Previous studies advise the > 250 μm fraction in high-Arctic sediments as iceberg IRD (Darby et al., 2006), and > 63 μm fraction as sea ice IRD (Spielhagen et al., 2004). However, others note that whether IRD is iceberg IRD or sea ice IRD can only be determined based on the content of the > 63-μm fraction (Polyak et al., 2010). Studying the grain size of modern surface sediments in the study area and their genesis can provide insight into distinguishing the causes of IRD and reconstructing the paleoceanographic environment recorded by IRD.

In the past decades, surface sediments in the Bering Sea and western Arctic Ocean have been studied. The content of grain size class (gravel, sand, silt, and clay), mean diameter, and sorting coefficient of the surface sediments from the Bering Sea and Chukchi Sea Shelf have been reported (Grebmeier et al., 1989; Feder et al., 1994). The GSDs of the Bering Sea and Arctic Ocean sediments are polymodal in nature (Nagashima et al., 2012; Dong et al., 2017), and exhibit regional characteristics (Darby et al., 2009; Park et al., 2014a). Additionally, the diameters of the particles in surface sediments are consistent with those of the particles in sea ice (Darby et al., 2009). However, these studies fail to systematically compare the spatial distribution patterns of different grain-size populations of sediments in the Bering Sea and western Arctic Ocean, as well as the sources and transport paths reflected by these patterns.

In this study, the GSDs of surface sediments obtained from the Bering Sea and the western Arctic Ocean were partitioned into populations with log-normal distribution function. Additionally, the spatial variations in the populations were compared, and their sources and transport trends were analyzed. Moreover, the driven forces of IRD in high-Arctic sediments was analyzed and its application to paleoceanography study was discussed.

2 Regional setting

The study areas are located in the Bering Sea and western Arctic Ocean, including the Bering Sea Shelf, Chukchi Sea Shelf, Canadian Basin, Chukchi Borderlands, Alpha Ridge, and Makarov Basin (Figure 1a). The northeastern region of the Bering Sea is a continental shelf where the water depth increases to the west and southwest. The Chukchi Sea has an average depth of 77 m, which is connected to the Bering Sea in the south via Bering Strait. The Herald Shoal and Hanna Shoal in the middle of and the northeast of Chukchi Sea, respectively, create three northward-trending channels: the Herald Valley and Hope Valley, the Central Channel, and the Barrow Canyon, respectively from west to east. In the high north of the Chukchi Sea, the ridges and plateaus are interlaced with basins.

The northern Bering Sea and western Arctic Ocean are affected by several oceanic currents. There are three branches of northward and northwestward currents over the Bering Sea Shelf, which are the Alaskan Coastal Water on the east side, the Bering Shelf Water in the middle, and the Anadyr Water on the west side (Figure 1a). These three currents are not fully mixed after flowing through the Bering Strait (Woodgate et al., 2015). The Alaskan Coastal Water continues to flow northward along the coast of Alaska and enters Arctic Basin through Barrow Canyon. After the Anadyr Water and Bering Shelf Water enter the Chukchi Sea, steered by terrain, one branch turns

northwestward first in the Hope Valley, and then flows northward through Herald Valley, and another branch flows northward through the Central Channel (Grebmeier et al., 2006). A portion of those two branches turn eastward after flowing through the valleys in the north Chukchi Sea, and converges with the Alaskan Coastal Current, and the remainder continues northward and into the Arctic Basin (Weingartner et al., 2005) (Figure 1b). In the Canadian Basin, the surface layer consists of the Beaufort Gyre, and the subsurface layer consists of the Atlantic Water. The flow directions of these two oceanic currents are opposite to each other. Eddies occur at the margin of the Chukchi Shelf, which laterally transports sediments into the Canadian Basin (O'Brien et al., 2013; Watanabe et al., 2014).

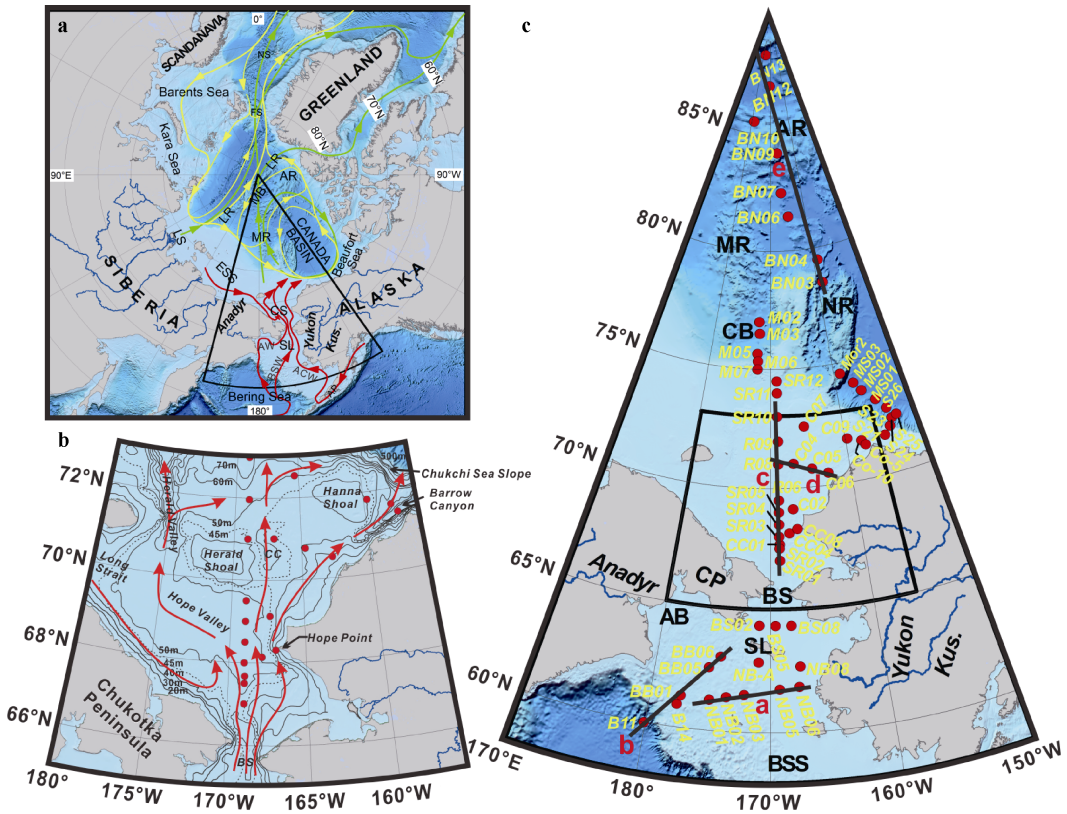

Figure 1 Oceanographic setting and location map of samples. Topography map (Jakobsson et al., 2012), major surface currents (red and green arrows) and intermediate water circulation (yellow arrows) in the Arctic Ocean (**a**). Topography, currents and locations of surface sediment samples in the Chukchi Sea (**b**). Locations of surface sediment samples (**c**). Black solid lines indicate the locations of the transects for grain size population comparison in Figure 5 to Figure 8 and Figure 10. Abbreviations in maps: ACW, Alaskan Coastal Water; AR, Alpha Ridge; AW, Anadyr Water; BS, Bering Strait; BSW, Bering Shelf Water; CB, Chukchi Basin; CC, Central Channel; CP, Chukchi Peninsula; CS, Chukchi Sea; ESS, East Siberian Sea; FS, Fram Strait; LR, Lomonosov Ridge; LS, Laptev Sea; MR, Mendeleev Ridge; NR, Northwind Ridge; SL, St. Lawrence Island.

The Yukon River delivers 55 × 10^6 T of sediments to Bering Sea per year, followed by Anadyr River which transport 8 × 10^6 T of sediments per year (VanLaningham et al., 2009). Sediment is delivered to the Chukchi Sea by local river discharge, coastal erosion, and the Bering Sea inflow, and is redistributed on the shelf by bottom erosion and redeposition (Viscosi-Shirley et al., 2003; Darby et al., 2009; Park et al., 2014a). Approximately one-third of the sediments from the Yukon River are transported by the northward oceanic current to the Chukchi Sea (Asahara et al., 2012). In addition, several moderate and small rivers in northwestern Alaska transport sediments to the Chukchi Sea, but the quantity of such sediments is not clear.

The sea ice in the study areas waxes and wanes with the change in seasons. In winter, sea ice expands close to the edge of the Bering Sea Shelf; in summer, it shrinks back close to the margin of the Chukchi Sea Shelf. Affected by barometric and sea level pressure, the sea ice in Bering and Chukchi seas drift westward, which form broad polynyas between the drift ice and fast ice adjacent to coast (Weingartner et al., 1998; Eicken et al., 2005; Serreze et al., 2016). The sea ice in Canadian Basin rotates clockwise pushed by the Beaufort Gyre and the wind field, and a portion of it enters the Nordic Sea through the Fram Strait with the Transpolar Drift (Stein, 2008). Particles in the "dirty ice" become an important sedimentary source and sedimentary mechanism in the western Arctic Ocean along with the drifting and melting of sea ice (Eicken et al., 2005).

3 Materials and methods

In this study, surface sediments were collected using box-cores at 59 locations in the Bering Sea and western Arctic Ocean during the 4th Chinese National Arctic Research Expedition in 2010 (Figure 1). Samples were successively treated with 10–30 mL of 30% H_2O_2, 30 mL of 10% HCl, 20 mL of 1 mol·L^{-1} Na_2CO_3 for removing organic matter, biogenic carbonates, and biogenic silica, respectively. De-ionized water (2000 mL) was added and kept for 24 h to rinse acidic ions. The sample residue was dispersed with 10 mL of 0.05 mol·L^{-1} $(NaPO_3)_6$ on an ultrasonic vibrator for 10 min before grain-size measurement. The GSDs of all samples were determined with a Malvern MasterSizer 2000 laser particle analyzer at the Third Institute of Oceanography, Ministry of Natural Resources. The MasterSizer 2000 has a measurement range of 0.02–2000 μm in diameter and a grain-size resolution of 0.166φ in interval ($\varphi = -\log_2(D)$, where D is grain diameter in mm), and therefore yields 100 grain-size fractions for every sample. The relative error of repeat test is < 3%.

A log-normal distribution function was applied to fit and partition the GSDs using the GrainAnalysis software. The software yields the optimum fitting of the measured GSD. A low value of fitting residual indicates better fitting results (Qin et al., 2005; Xiao et al., 2012).

4 Results

4.1 Spatial variability of sediments

The grain-size measurement results showed that sediments on the northeastern Bering Sea Shelf are the coarsest, with the highest sand content, and became finer westward. Sediments on the southern Chukchi Sea and near the coast of Alaska were also relatively coarser and became finer towards the west. The sediments from the high Arctic were relatively fine with the highest clay content (Figure 2).

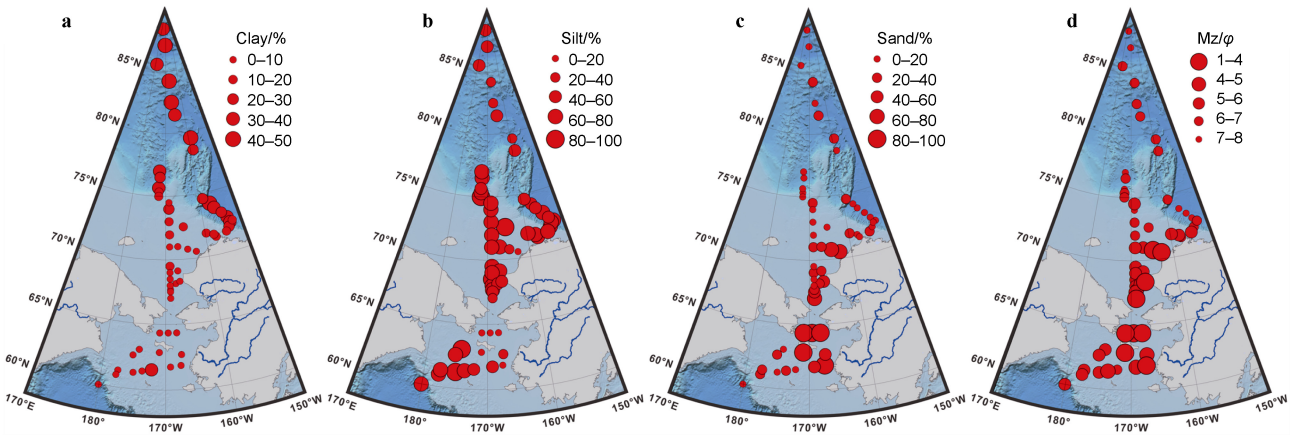

Figure 2 Spatial variability in percent content of clay, silt, and sand fractions (**a**–**c**) and mean grain size of surface sediments (**d**).

Based on Folk's classification (Folk, 1954), the surface sediments in the study area can be classified into six textural types, namely, mud, sandy mud, silt, sandy silt, silty sand, and sand (Figure 3). Mud was found at four stations, located in the Chukchi Basin (stations M02 and M05) and at the base of the Chukchi Sea Slope (stations MS03 and MS26). This type of sediment was dominated by silt (> 50%), followed by clay (> 30%), and the sand content was < 10%. Sandy mud was mainly found in the high Arctic at stations with names preceded by BN (such as BN03 and BN04), as well as at stations at the base of the Chukchi Sea Slope (such as MS02 and MOR2). This type of sediments consisted mainly of silt (36%–53%) and clay (27%–42%), and the sand content ranged from 10%–23%. Sandy silt was found mainly on the western Bering Sea Shelf (B11 and BB05) as well as the Chukchi Sea Shelf far from the Alaska coast (C09 and R09). This type of sediment consisted of silt (60%–81%), sand (10%–48%), and clay (3%–18%). Silt was found mainly on the central-northern Chukchi Sea Shelf (C07 and SR10), in the Chukchi Basin

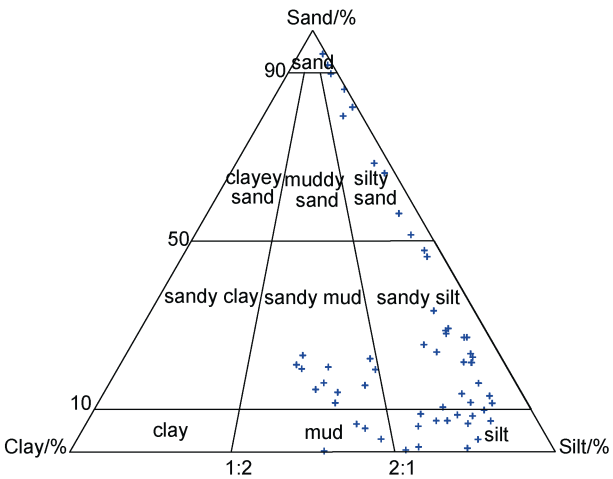

Figure 3 Folk's ternary diagram of textural types of surface sediments.

(M03 and M07), and at the base of the Chukchi Sea Slope (MS01 and S24). This type of sediment was dominated by silt (67%–84%), followed by clay (9%–31%), and the sand content was less than 10%. Silty sand and sand were found on the northeastern Bering Sea Shelf, Bering Strait, and near the coast of Alaska (NB06, BS08, and CC8). The sand content in these two types of sediments were > 50% with almost no clay (< 5%) in sediments.

4.2 Characteristics of GSD and its populations

Based on the GSD fitting results, sediments of the 59 stations in the study area are composed of 2–5 populations. The majority of these sediments consist of 3–4 populations, and a few samples consist of 2 or 5 populations. For the convenience of discussion, the populations in GSDs are named as C1, C2, C3, C4, and C5 according to their mode diameters (MD) from fine to coarse. The MD is the most frequently occurring particle size in a population of grains. Figure 4 shows the representative GSD and their populations of sediments from the study areas. Based on the number of populations in GSD, the GSDs of sediments from the study area are categorized into four basic types, namely, GSD II, GSD III, GSD IV, and GSD V. The characteristics of each GSD type and its populations are described below.

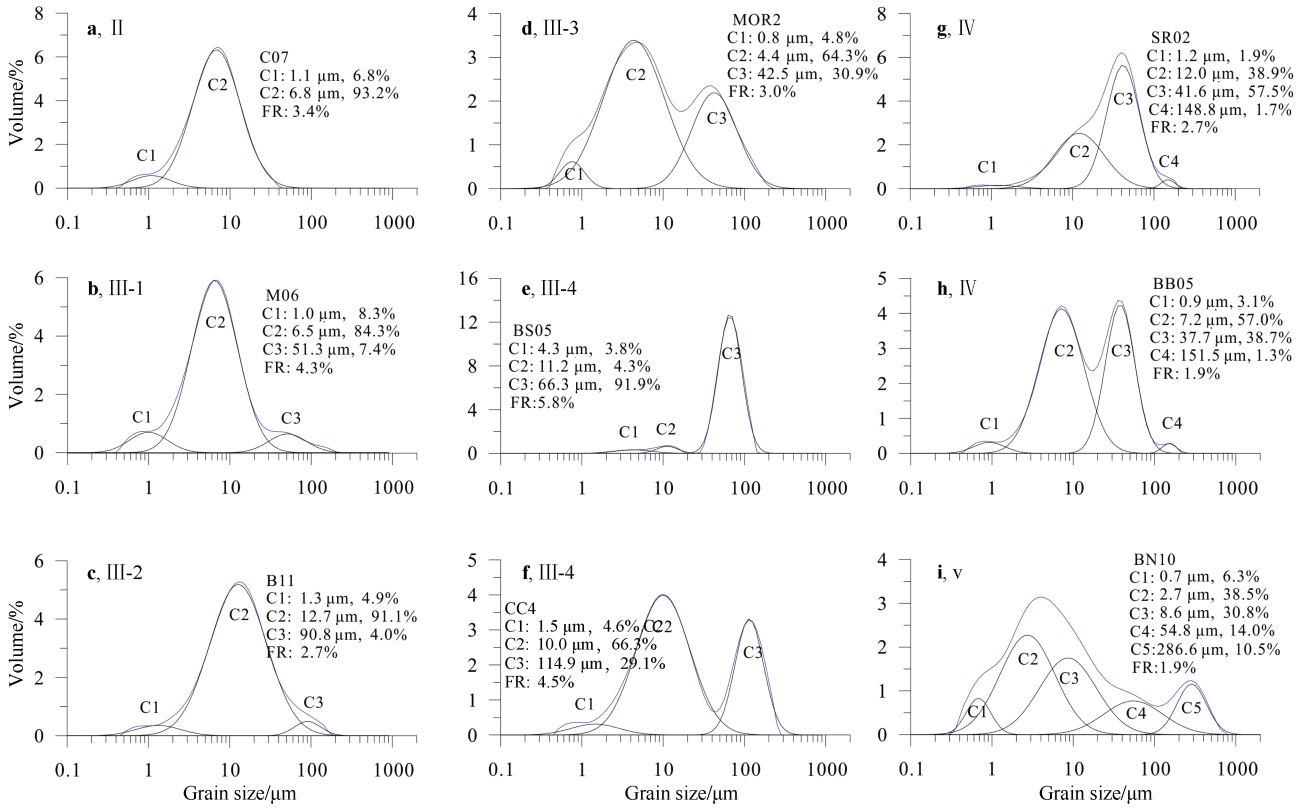

Figure 4 Representative GSDs and their populations. II (**a**), III-1 (**b**), III-2 (**c**), III-3 (**d**), III-4 (**e**, **f**), IV (**g**, **h**), and V (**i**) are GSD types; C1, C2, C3, C4, and C5 are populations from fine to coarse in GSD. FR is fitting residual.

Sediments with GSD II consist of two populations (Figure 4a), in which the content of C1 (MD: 1 μm) is < 12% and C2 (MD: 3–7 μm) is over 87%. The textural type of the sediments is mud or silt. Only four samples (C07, SR11, S24, and MS03) exhibit GSD II, which were located in the central-northern Chukchi Sea and at the base of the Chukchi Slope.

Sediments with GSD III are composed of three populations, and the MD of its C1 and C2 is similar to those of GSD II. Based on the relative content of the C2 and C3 as well as the MD of the C3, GSD III can be further categorized into four subtypes, namely III-1, III-2, III-3, and III-4. For GSD III-1, the content of C2 was much higher than that of C1 and C3, and the MD of C3 was approximately 40 μm (Figure 4b). Sediments with GSD III-1 are located on the southwestern Bering Sea Shelf (B14), in the Chukchi Basin (M02, M05, M06, and M07), and the base of the Chukchi Sea Slope (MS01, S25, and S26), and the textural type of the sediments is mud, silt, or sandy silt.

The shape of GSD III-2 is similar to that of GSD III-1. However, the MD of C3 in GSD III-2 ranges from 80–120 μm, coarser than that of GSD III-1 (Figure 4c). Sediments with GSD III-2 are located at western Bering Sea Shelf (B11 and NB01), the Chukchi Sea Shelf near Barrow Canyon (Co-10 and Co-5), and the northern Chukchi Sea Shelf (SR12), and the sedimentary textural type is silt or sandy silt.

If the content of C3 in GSD III-1 and GSD III-2 increased dramatically, the GSD would transform into GSD III-3 and GSD III-4, respectively. The GSD III-3 is notably coarse-skewed or bi-modal due to the dramatic increase in C3 (Figure 4d). Sediments with GSD III-3 were obtained from the base of the Chukchi Sea Slope (MS02 and MOR2) and the sedimentary textural type is sandy mud. Two samples, collected at NB02 and SR04, exhibited the characteristics of GSD III-3; however, the MD of their C3 is approximately 18 μm, finer than that of the GSD III-3 previously mentioned, whose MD of C3 is approximately 40 μm (see Figure 5). The GSDs of sediments from those two stations can be treated as special cases of GSD III-3.

The C3 of GSD III-4 has an MD of 40–160 μm, wider range, and is coarser than that of GSD III-3 (Figure 4e). Additionally, the C3 content of GSD III-4 is > 60%, and the maximum is up to 95%. Sediments with GSD III-4 are located at the northeastern Bering Sea (NB06, NB08, and NB-A), Bering Strait (BS02, BS05, BS08, and SR01), and near the Alaskan coast (C05 and C06), and its sedimentary textural type is silty sand or sand. The sediments at station CC4 near the Alaskan coast exhibited a bi-modal GSD pattern similar to that of GSD III-3 (see Figure 4f). However, its MD of C3 is > 100 μm; thus, the GSD curve of this sediment sample can be treated as a special case of GSD III-4.

Sediments with GSD IV contained four grain-size populations. The GSD IV is a result of mixing of sediments with GSD III-1 and GSD III-2. The MDs of C1, C2, C3, and C4 of the GSD IV sediments are approximately 1 μm, 10 μm, 40 μm, and > 100 μm, respectively. Due to the shift in the relative content of the C2, C3, and C4, GSD IV represents fine-skewed, coarse-skewed, or bi-modal distributions, as shown in Figures 4g and 4h. Sediments with GSD IV are the most common in the samples obtained from the study area and have the most diverse textural types, including mud, sandy mud, silt, sandy silt, and silty sand, which is obtained from Bering Sea Shelf or Chukchi Sea Shelf.

Sediments with GSD V are composed of five grain-size populations, and the MDs of C1 to C5 are < 1 μm, 2–4 μm, 8–15 μm, 50–80 μm and > 200 μm, respectively, as shown in Figure 4i. Sediments with GSD V are located in the high Arctic, and its sedimentary textural type is sandy mud.

5 Discussion

5.1 Deposition mechanisms on the Bering Sea Shelf

Sediments from the northeastern Bering Sea Shelf and the Bering Strait exhibit a GSD III-4 pattern, which is a typical characteristic of river origins, and its dominant population (C3) is the result of bedload transport (Sun et al., 2002; Xiao et al., 2012). Therefore, it is inferred that sediments with GSD III-4 from the northeastern Bering Sea Shelf originated from the Yukon River. Figure 5 shows the GSDs and its populations on a near east-west transect on the Bering Sea Shelf (see Figure 1 for the location). The surface sediments at NB06 outside the Yukon River estuary consist mostly of C3 with a content up to 95% and an MD of approximately 63 μm. Toward the west-southwest direction, the MD of C3 in sediments decreased gradually. At NB02 on the central-western Bering Sea Shelf, the MD of C3 decreased to 52 μm and its content decreased to 64%. Further westward to NB01, owing to C3, it further decreased in size and the C2 content increased; the C2 and C3 from the Yukon River merged into a new population that was coarser than the C2 and finer than the C3 of other samples on the transect. Moreover, the content of the fine grain-size populations (C1 + C2) representing particles transported by suspended loads on thetransect increased from < 5% outside of Yukon River estuary to 98% on the central-western Bering Sea Shelf.

Westward along the transect in Figure 5, the sediments exhibit a trend of being finer, more poorly sorted, and more negatively skewed. Although this type of trend was not a case used in sediment trend analysis (Gao and Collins, 1992; Le Roux and Rojas, 2007; Poizot and Méar, 2008), when sediments become finer, the skewness tends to become more negative and they can become more poorly sorted (Poizot et al., 2008). The variations in content and the MD of C2 and C3 in the transect and the distribution of grain size parameters (see in Figure 3) indicate that the sediments originating from the Yukon River disperse westward.

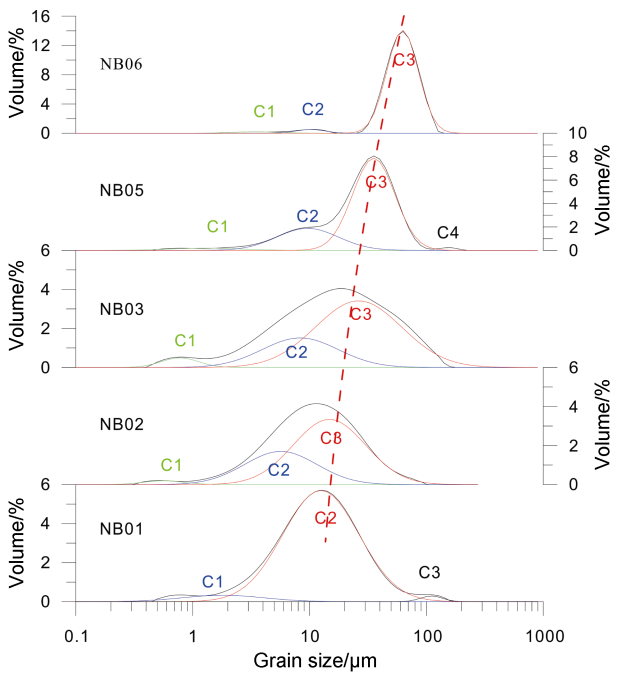

Figure 5 Variations in GSDs and its populations of sediments in the southern Bering Sea Shelf on an east-west transect (see line a in Figure 1c for the location of the transect and sample names), the red dashed line represents the spatial variation trend in the C3.

The GSD patterns of sediments at the south and north sides of St. Lawrence Island (NB-A, BS02, BS05 and BS08) are similar to those of the sediments outside the Yukon River estuary, indicating that the sediments there also originated from the Yukon River. However, due to a shallow water depth and an increased velocity of ocean currents, the fine fractions in the sediments were re-suspended or winnowed by the waves and currents (Nagashima et al., 2012), which resulted in the sediments with GSD III-4 in these regions that have an extremely low C1 and C2 content and consist mainly of C3.

The GSD and populations of the sediments outside of Anadyr Bay differed from those of the sediments originating from the Yukon River. Sediments from this region exhibited GSD III-1, III-3, or V patterns. C2 dominated in the sediments followed by C3 (Figure 6). As shown in Figure 6, C2 became finer from south to north. Combined with the variation trend of C2 in Figure 5, it can be inferred that this population dispersed westward from the Yukon River first and was then transported northward from the edge of the continental shelf. The content of C3 was the highest and the grain-size was the coarsest outside of Anadyr Bay (BB05) and decreased northward and southward. It is unlikely that the C3 in sediments outside Anadyr Bay originated from the Yukon River. As shown in Figure 5, the C3 on the central Bering Sea Shelf was already finer than that of the sediments at BB05. Therefore, it can be inferred that the C3 in sediments on the western Bering Sea Shelf originated from the Anadyr River. Some sediments from the west side of the Bering Sea Shelf (BB01, BB05, and BB06) exhibited an extremely low content of C4 with MD > 100 μm (Figure 6), which were possibly formed from IRD.

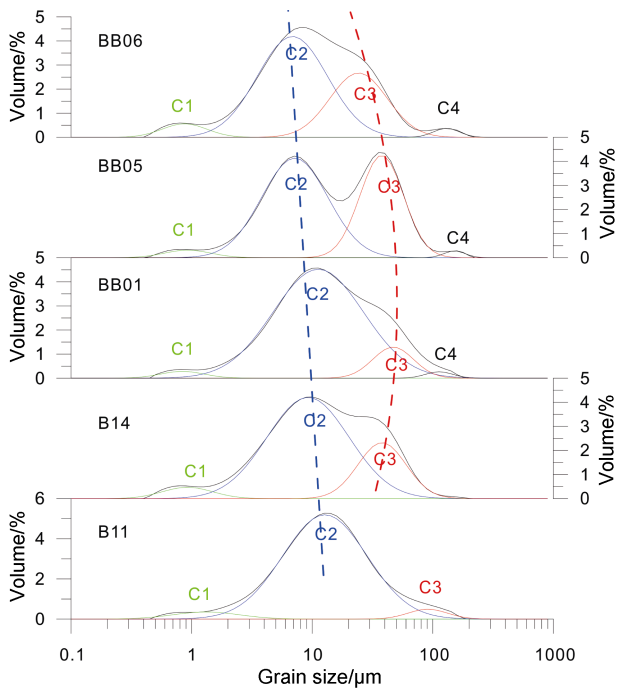

Figure 6 Variations in GSDs and populations in sediments on the western Bering Sea Shelf on a south-north transect (see line b in Figure 1c for the location of transect and sample names). The blue and red dashed lines indicate the spatial variation trends of C2 and C3, respectively.

The sediments contributions of the Yukon River and Anadyr River on the Bering Sea shelf implied by GSDs and its populations are mutually corroborated with evidence from previous research, such as results of geochemistry and minerals. The isotopes of Sr and Nd, and the spin resonance intensities and crystallinity indices of quartz indicate that the sediments on most of the northern Bering Sea Shelf originated from the Yukon River, and that the silty sand and sandy grain-size fractions in sediments outside Anadyr Bay originated from the Chukotka Peninsula (Asahara et al., 2012; Nagashima et al., 2012). Clay mineral assemblages and distribution patterns have shown that the clay from the Yukon River disperses westward and northward (Nwaodua et al., 2014). Furthermore, magnetic mineral data have demonstrated a difference in the material source between the east and west sides of the northern Bering Sea Shelf (Wang et al., 2014). It is not difficult to understand the south-to-north sediment transport trend in this case, because all three ocean currents on the shelf flow northward or northwestward on the Bering Sea Shelf.

5.2 Deposition mechanisms on the Chukchi Sea Shelf

Figure 7 shows the variation in GSDs and its population of surface sediments on the Chukchi Sea Shelf approximately along the 169°W meridian. Different variation trends can be found for the C2 and C3 of sediments on the transect divided by station SR04. South of SR04, the C3 became notably finer towards the north and the C2 also became slightly finer northward. However, north of SR04, there was no significant change in the MD of C2, but the MD of the C3 increased towards the north.

Like the sediments on the northern Bering Sea Shelf that originated from the Yukon River, sediments on the southern Chukchi Sea adjacent to the Bering Strait (SR01 and SR02) also exhibited a GSD III-4 pattern, implying that the sediments in the southern Chukchi Sea also originated from the Yukon River. The northward finer trend of C2 and C3 in sediments on the southern Chukchi Sea was a result of sedimentary differentiation due to the velocity decrease in sediment load currents after entering the Chukchi Sea.

Approximately one-third of the sediments input by the Yukon River enters the Chukchi Sea (Asahara et al., 2012). According to the variation trends of populations on the transect shown in Figure 7 and Figure 8, it is inferred that coarse particles (C3) in sediments originating from the Yukon River were deposited in the Hope Valley, in the southern Chukchi Sea due to sedimentary differentiation. The ocean color satellite images shows a portion of sediments originating from the Yukon River flows into the

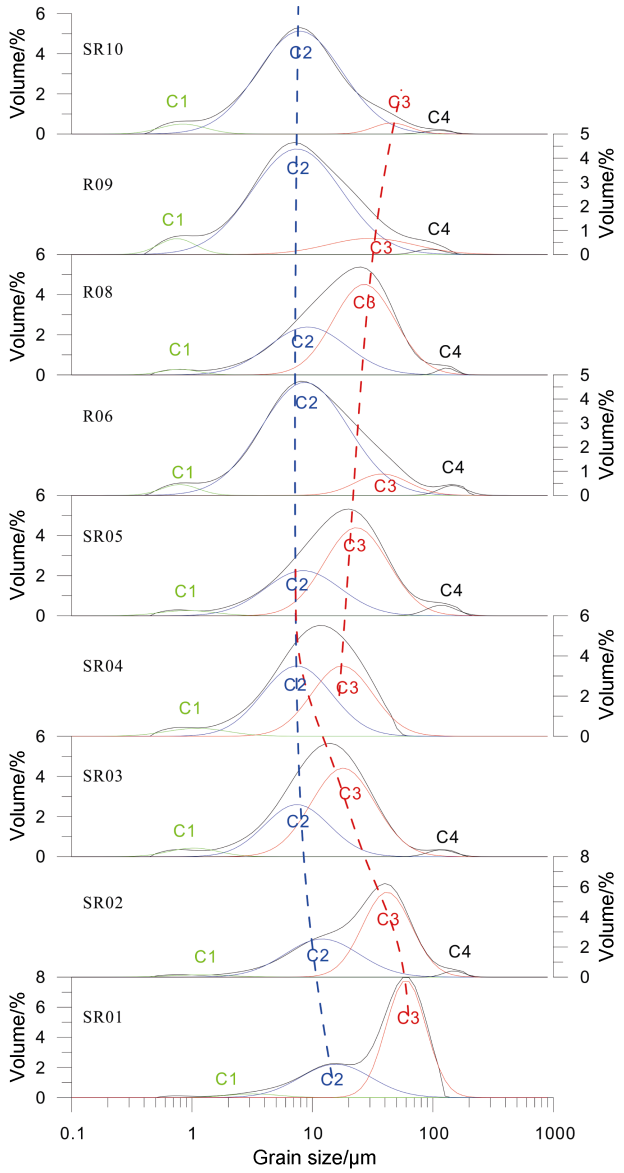

Figure 7 Variations in GSDs and its populations in sediments on a south-north transect approximately along the 169°W meridian (see line c in Figure 1c for the location of transect and samples). The blue dashed line shows the spatial variations in C2. The red dashed line shows the spatial variations in C3.

Hope Valley (Woodgate et al., 2015) (Figure 9); however, the finer particles could be transported further north by currents. Clay mineral data have shown that sediments originating from the Yukon River enter the Arctic basins (Asahara et al., 2012). After the two currents flow through the Herald Valley and the Central Channel, a portion of those two currents turn eastward, and converge with the Alaskan coastal current, which also flows into the high Arctic. Thus, the fine particles originating from the Yukon River, including C1 and C2 in sediments, enter the central-northern Chukchi Sea Shelf. The variation in C2 shown in Figures 7 and 8 indicates that the C2 in sediments on the central-northern Chukchi Sea Shelf are both from the

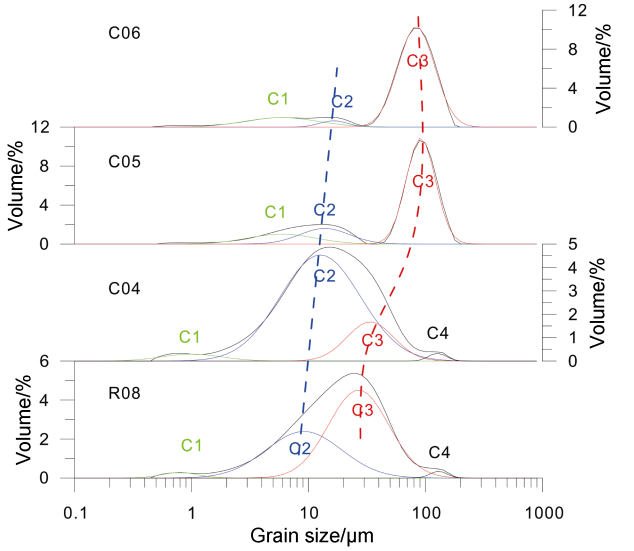

Figure 8 Variations in GSDs and its populations in surface sediments from the Chukchi Sea Shelf on an east-west transect (see line d in Figure 1c for the location of transect and samples). The blue and red dashed lines show the spatial variation in C2 and C3, respectively.

Yukon River and Alaska. This is corroborated by clay mineral evidence, which demonstrates that the Chukchi Sea Shelf contains matter originating from both the Bering Sea and terrigenous Alaska (Naidu et al., 1982; Viscosi-Shirley et al., 2003).

The coarsening of the C3 north of SR04 on the transect shown in Figure 7 indicates that C3 does not originate from the Yukon River. A comparison of the GSDs of sediments on the Chukchi Sea Shelf in the east-west direction (Figure 8) shows that both C2 and C3 become coarser from the central shelf to the coast of Alaska. Previous results with high-density surveys have demonstrated that sediments become finer from coast to sea (Feder et al., 1994), which is consistent with the results in this study. It is therefore inferred, that the C3 in sediments on the central Chukchi Sea Shelf, north of SR04 originated from Alaska to the east or from the Beaufort Sea Shelf instead of the Yukon River.

It has been found that sediment-loaded sea ice drifts northwestward from the coast of Alaska to the central continental shelf and that sediments in the sea ice consist of fine silt and clay fractions, and occasionally fine sand and coarse silt fractions (Tucker et al., 1999; Eicken et al., 2005; Serreze et al., 2016). A zone of surface sediments with coarse coal fragments extends northwestward from the coast of Alaska. Those coal fragments were from the Mesozoic strata in Alaska (Zhang et al., 2019). Mineral assemblages in IRD, Sr, and Nd isotopes in sediments have shown that sediments on the central-northern Chukchi Sea Shelf contain particles originating from the land to its east (Darby, 2003; Asahara et al., 2012). Local rivers and coastal cliff dumping in northwestern Alaska can ensure the sources of material transported by sea ice to the central continental

shelf. These sediments are selectively entrained and released to the continental shelf by sea ice (Reimnitz et al., 1998). In winter, driven by north-easterly wind, westward currents from the coast to the continental shelf result in an expansion of the polynyas along the coast of Alaska (Weingartner et al., 1998), which is favorable for the entrainment of resuspended clay-silty particles by sea ice (Eicken et al., 2005). Sediments in frazil ice formed in the polynyas are finer than bottom sediments under the polynyas. As a result of these selective entrainments, seabed sediments under the polynyas become coarser. Due to the melting of sea ice and relatively fine sediments released with the sea ice melting, sediments on the central-northern Chukchi Sea Shelf grow finer from the coast to the sea.

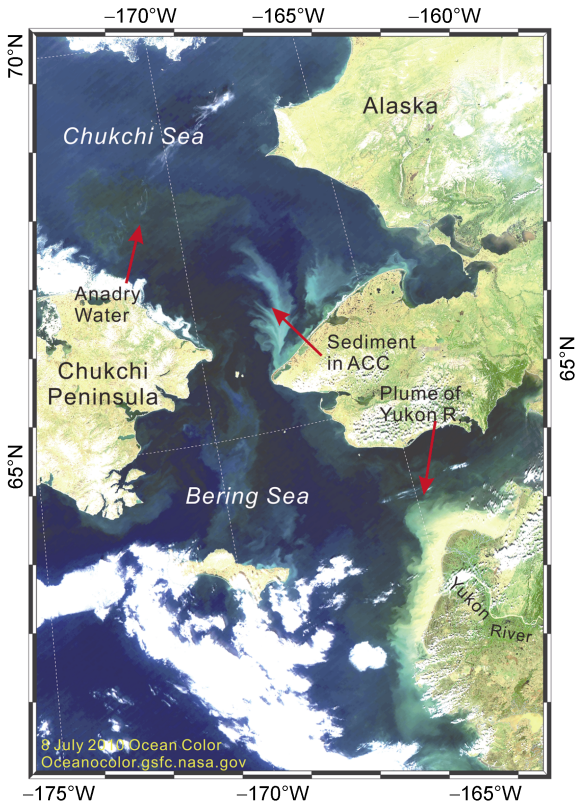

Figure 9 Ocean color image of Bering Sea and Chukchi Sea (http://oceancolor.gsfc.noaa.gov). The sediment plume of Yukon River moves northward, and the plume transported by Alaskan Coastal Current (ACC) turns westward and into Hope Valley after through the Bering Strait.

Anchor ice could freeze seabed sediments inside it; however, it mostly melts in the source regions, and consequently, its role in the sediment transport is relatively unimportant (Nürnberg et al., 1994; Reimnitz et al., 1998; Eicken et al., 2005). Additionally, the formation of coastal fast ice and frazil ice results in an increase in seawater salinity (brine water), which subsequently flows down along the seabed to the east of the Herald Shoal on the central Chukchi Sea Shelf (Weingartner et al., 1998). The flow of brine water near the seabed can also transport fine sediments westward.

A portion of the surface sediments on the central Chukchi Sea Shelf also contained a C4 with an MD of > 100 μm, but the content was extremely low. This population is likely coarse IRD related to sea ice.

5.3 Deposition mechanisms at the Chukchi Sea margin

Most sediments collected from the Chukchi Basin and the base of the Chukchi Sea Slope (M02, M05, M06, M07, MS01, S25, and S26) exhibit the GSD III-1 pattern, a few samples (MS02, MS03, and S24) exhibit the GSD II or GSD III-3 pattern, and sediments from some stations (M03, S21, and S23) exhibit the GSD IV pattern due to the presence of C4 with an MD of > 100 μm. The C2 content of sediments in this region is significantly higher than the content of any other populations. In addition, this C2 has an MD of 3–8 μm (mostly ~5 μm), which is notably finer than the MD of C2 in sediments on the Chukchi Sea Shelf, where it was mostly > 8 μm. The MDs of C3 and C4 (if any) of sediments in Chukchi Basin and at the base of the Chukchi Sea Slope were close to those of C3 and C4 of sediments on the central Chukchi Sea Shelf, which ranged from 30–50 μm and 100–200 μm, respectively.

Fine particles in sea ice split into three fractions, namely, < 0.5, 2, and 5 μm. The < 0.5 μm and 2 μm fractions resulted from suspension freezing and anchor ice formation, respectively, and the 5 μm fraction was entrained both by suspension freezing and anchor ice (Darby et al., 2009). The MD of the C2 in sediments from the Chukchi Basin and the base of the Chukchi Sea Slope was close to that of the 5 μm fraction in sea ice, indicating that at least some portion of particles in the sediments there, was deposited from melting ice. Sediments from the Chukchi Basin and the base of the Chukchi Sea Slope did not contain the < 0.5 μm and 2 μm fractions found in sea ice, but only a C1 with an MD of 0.7–1.1 μm, which was found between 0.5 and 2 μm, suggesting that the finest C1 in sediments from this region was mixed with particles from other sources. The fine clay fraction may be suspended by weak currents or may act as colloidal material maintained in suspension for long distances and over long periods of time (Darby et al., 2009). Additionally, the contents of < 0.5 μm and 2 μm fractions in sea ice were also relatively low. During the process in which sea ice melted and the particles in the sea ice settled to the seabed, the < 0.5 μm and 2 μm fractions might be mixed with the suspended clay that originally existed in the water column to form a merged population with an MD of 0.5–2 μm.

The C3, with an MD of 30–50 μm in surface sediments from the Chukchi Basin and the base of the Chukchi Sea Slope, also exists in the core sediment from the margin of the Chukchi Sea Shelf (Darby et al., 2009). This population represents down-slope and along-slope sediment transports in response to local bottom currents (Darby et al., 2009).

Ice-tethered and mooring sediment trap data have demonstrated the existence of lateral transport of suspended particles in the Chukchi Borderland. Shelf-break eddies propagating north of the Chukchi shelf break can transport re-suspended sediments to the high Arctic Ocean (O'Brien et al., 2013; Watanabe et al., 2014). Additionally, lateral transport by density flows and by the benthic nepheloid layer flowing along the seafloor cannot be excluded (O'Brien et al., 2006; Hwang et al., 2008; Darby et al., 2009; Honjo et al., 2010). Lithogenic particles found in sediment traps are clay and silt and rarely contain coarse-grained IRD. However, due to a lack of grain-size analysis data for sediments in traps, it is impossible to compare the grain sizes of particles laterally transported by local currents and particles of sediments in their affected regions.

The contribution of sea ice cannot be excluded as the cause of C3 in sediments from the Chukchi Sea Basin and the base of the Chukchi Sea Slope. This is because IRD with a diameter similar to that of C3 has also been found in anchor ice (Darby et al., 2011). However, the contribution of anchor ice to Arctic sediments currently remains unknown. Therefore, the origin of the C3 in sediments from the Chukchi Basin and at the base of the Chukchi Sea Slope requires further investigation.

Surface sediments from the Chukchi Basin and the base of the Chukchi Sea Slope contains an extremely low content of the C4 with an MD of > 100 μm, which was IRD originated (Eicken et al., 2005; Darby et al., 2011).

5.4 Characteristics of coarse-grained IRD in the high Arctic Ocean

Sediments collected from the eight stations in the high Arctic Ocean exhibit a polymodal GSD pattern and consisted of five populations except for the BN04 sample (Figure 10). Clay and silt accounted for a major portion of these sediments. The MD of C1 and C2 is < 1 μm and 2.4–4 μm, respectively. The C3 had an MD of 7–15 μm and was mostly < 10 μm. The high Arctic Ocean is beyond the region affected by eddies. Some samples in this study were collected from ocean ridges, where the near-bottom nepheloid layers and turbidities do not reach. The GSDs of surface sediments in the high Arctic Ocean are similar to those of sea ice-deposited sediments in the central Arctic Ocean (Clark and Hanson, 1983). Additionally, the MD of the fine population is comparable to that of fine IRD in sea ice (Darby et al., 2009). Considering the differences between the different analytical methods and instruments, the MD of C2 in sediments from the high Arctic Ocean in this study is on the same order of sea ice-deposited sediments with a peak diameter of 8 φ–9 φ (1.95–3.9 μm) (Clark and Hanson, 1983) and sea ice IRD with an MD of 5 μm (Darby et al., 2009). The C3 in sediments from high Arctic Ocean likely corresponds to the grain-size fraction with a peak diameter of 7 φ–8 φ (3.9–7.8 μm) in IRD sediments from the Beaufort Sea and the central Arctic Ocean (Reimnitz et al., 1998).

The sandy C4 and C5 in surface sediments from the high Arctic Ocean is the most distinguishing feature that sets them apart from those obtained from other parts of the study area. The C4 and C5 have MDs of 50–90 μm and 200–400 μm, respectively. Particles of 50–90 μm diameter are common in dirty ice and are considered the cause of anchor ice formation (Darby et al., 2011), and particles with diameters of 100 and 250 μm have been discovered in sea ice in the Beaufort and Chukchi Sea Shelf margins and the central Arctic Ocean (Reimnitz et al., 1998; Eicken et al., 2005).

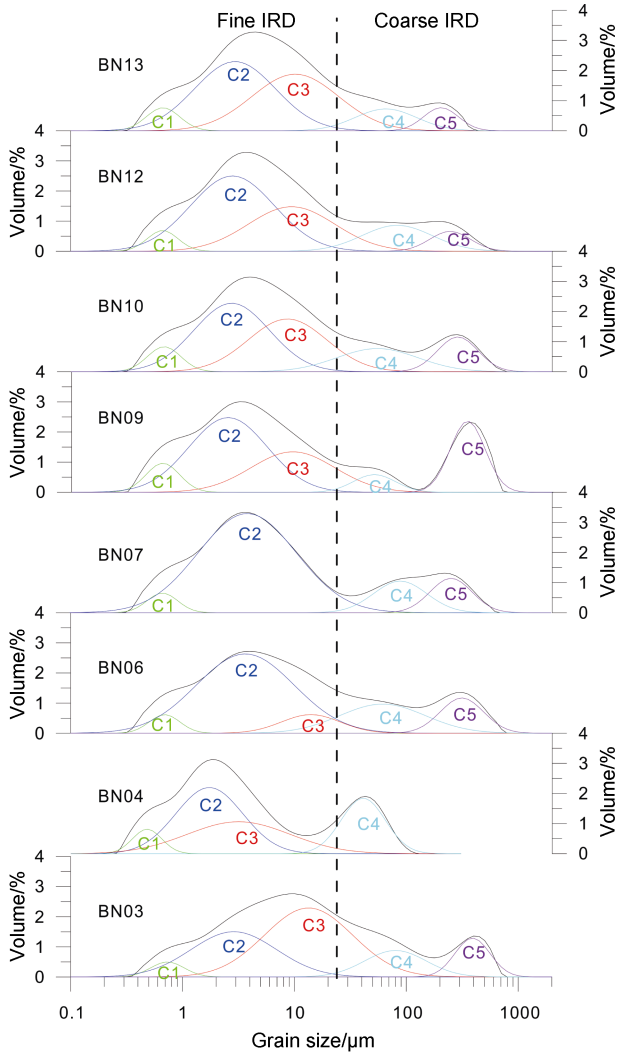

Figure 10 Variations in GSDs in the population of sediments from the high Arctic Ocean on the near south-north transect (see line e in Figure 1c for the location of transect and samples). To the right of the black dashed line are two coarse populations with diameters > 63 μm and > 250 μm.

Particles > 250 μm have been treated as iceberg IRD in paleoceanography research. In some cases, particles > 63 μm in sediments were similarly treated, whereas in other cases, they were treated as sea ice IRD. However, it is

difficult to distinguish the sea-ice IRD from the iceberg IRD because the particles in modern sea ice exhibit a similar GSD pattern to that in icebergs (Nürnberg et al., 1994). While it is difficult to accurately evaluate the contributions of iceberg IRD to modern sediments in the high Arctic Ocean, it can at least be confirmed that the contribution of iceberg IRD to surface sediments in the study area is unimportant because ice sheets surrounding the Arctic Ocean have shrunk sharply or disappeared since the Holocene. It is undeniable that sporadic icebergs from Greenland and the Canadian Arctic Archipelago can drift to the west Arctic Ocean if anomalous wind fields occur. Considering that the western Arctic Ocean in this study is currently covered by sea ice, sea ice should be the main contributor to C4 and C5 in sediments from the high Arctic Ocean.

The existence of C4 and C5 in surface sediments from the high Arctic Ocean is a common phenomenon throughout the glacial-interglacial cycles. The grain-size data from a core collected at station BN05 show that the sediments consisted of populations with diameters of approximately 4 μm, 7–7.5 μm, 85–95 μm and > 250 μm, and the two coarsest populations similar to C4 and C5 change in phase (Dong et al., 2017). This suggests that sediments in the central Arctic Ocean during the glacial-interglacial cycles have the same populations.

In view of the ubiquitous populations with a diameter of > 63 μm and > 250 μm, respectively, in surface and core sediments in the central Arctic Ocean, and the difficulty in distinguishing whether sea ice or icebergs are the sources, it is inadequate to use the grain-size fraction of > 63 μm or > 250 μm in sediments in the central Arctic Ocean as proxy indexes for the evolution of sea ice or ice sheets surrounding the Arctic Ocean. Other supplemental methods need to be used.

6 Conclusions

Based on the spatial variation in the GSDs and the populations, surface sediments on the northeast Bering Sea Shelf originated from the Yukon River and dispersed westward. The coarse population with an MD of 24–46 μm in sediments outside of the Anadyr Bay originated from the Anadyr River. The population with a diameter of approximately 10 μm in sediments on the west side of the Bering Sea Shelf was transported from south to north by currents and become finer northward.

The Yukon River sediments were transported into the Chukchi Sea and deposited mainly in Hope Valley, in the south Chukchi Sea. The sediment populations with MD > 10 μm and MD < 10 μm on the central Chukchi Sea Shelf originated from Alaska to its east, and the Bering Sea respectively.

The populations of sediments obtained from the Chukchi Basin and the base of the Chukchi Sea Slope differed from those of sediments from the Chukchi Sea Shelf and the high Arctic Ocean. Sediments there originated from sea ice IRD and particles laterally transported by eddies.

Most surface sediments collected from the high Arctic consisted of five populations. Apart from the fine populations that formed as a result of sea ice, two coarse populations with an MD of 50–90 μm and 200–400 μm, respectively, were ubiquitous in the Quaternary sediments in the high Arctic Ocean. It is impossible to distinguish sea ice IRD from iceberg IRD based on grain size alone. Therefore, caution should be exercised when reconstructing the evolution of ice sheets based on fractions > 63 μm or > 250 μm in sediments in the high Arctic Ocean; other supplemental methods must be used.

Acknowledgements We are grateful to the captain, crews, and scientists on board R/V *Xuelong* during the 4th Chinese National Arctic Research Expedition. We thank Profs. Jule Xiao and Xiaoguang Qin for providing the software, and Prof. Rujian Wang and Dr. Wenshen Xiao for providing data of sedimentary dynamics on the Chukchi Sea margin. This study was financially supported by the scientific research foundation of Third Institute of Oceanography, MNR (Grant no. 2018006), Chinese Polar Environment Comprehensive Investigation & Assessment Programmes (Grant no. 2016-03-02), and the National Natural Science Foundation of China (Grant nos. 41306205, 41876229).

References

Asahara Y, Takeuchi F, Nagashima K, et al. 2012. Provenance of terrigenous detritus of the surface sediments in the Bering and Chukchi seas as derived from Sr and Nd isotopes: Implications for recent climate change in the Arctic regions. Deep Sea Res Part II: Top Stud Oceanogr, 61-64: 155-171, doi: 10.1016/j.dsr2.2011.12.004.

Ashley G M. 1978. Interpretation of polymodal sediments. J Geol, 86(4): 411-421, doi: 10.1086/649710.

Clark D L, Hanson A. 1983. Central Arctic Ocean sediment texture: A key to ice transport mechanisms//Molnia B F. Glacial-Marine Sedimentation. Springer: Boston MA, 301-330, doi: 10.1007/978-1-4613-3793-5_7.

Darby D A. 2003. Sources of sediment found in sea ice from the western Arctic Ocean, new insights into processes of entrainment and drift patterns. J Geophys Res-Earth, 108(C8): 3257, doi: 10.1029/2002JC001350.

Darby D A, Myers W B, Jakobsson M, et al. 2011. Modern dirty sea ice characteristics and sources: The role of anchor ice. J Geophys Res, 116(C9): C09008, doi: 10.1029/2010jc006675.

Darby D A, Ortiz J D, Polyak L, et al. 2009. The role of currents and sea ice in both slowly deposited central Arctic and rapidly deposited Chukchi–Alaskan margin sediments. Glob Planet Chang, 68(1): 58-72, doi: 10.1016/j.gloplacha.2009.02.007.

Darby D A, Polyak L, Bauch H A. 2006. Past glacial and interglacial conditions in the Arctic Ocean and marginal seas– a review. Prog Oceanogr, 71(2): 129-144, doi: 10.1016/j.pocean.2006.09.009.

DeConto R, Pollard D, Harwood D. 2007. Sea ice feedback and Cenozoic evolution of Antarctic climate and ice sheets. Paleoceanography, 22(3): PA3214, doi: 10.1029/2006pa001350.

Dong L S, Liu Y G, Shi X F, et al. 2017. Sedimentary record from the Canada Basin, Arctic Ocean: implications for late to middle Pleistocene glacial history. Clim Past, 13(5): 511-531, doi: 10.5194/cp-13-511-2017.

Dunhill G. 1998. Comparison of sea-ice and glacial-ice rafted debris: grain size, surface features, and grain shape. Open-File Report. California: Menlo Park, 98-367.

Eicken H, Gradinger R, Gaylord A G, et al. 2005. Sediment transport by sea ice in the Chukchi and Beaufort seas: Increasing importance due to changing ice conditions? Deep-Sea Res Part Ⅱ: Top Stud Oceanogr, 52(24): 3281-3302, doi: 10.1016/j.dsr2.2005.10.006.

Fan D J, Qi H Y, Sun X X, et al. 2011. Annual lamination and its sedimentary implications in the Yangtze River Delta inferred from high-resolution biogenic silica and sensitive grain-size records. Cont Shelf Res, 31(2): 129-137, doi: 10.1016/j.csr.2010.12.001.

Feder H M, Naidu A, Jewett S C, et al. 1994. The northeastern Chukchi Sea: benthos-environmental interactions. Mar Ecol Prog Ser, 111: 171-190, doi: 10.3354/meps111171.

Folk R L. 1954. The distinction between grain size and mineral composition in sedimentary-rock nomenclature. J Geol, 62(4): 344-359, doi: 10.1086/626171.

Folk R L, Ward W C. 1957. Brazos River bar: A study in the significance of grain size parameters. J Sediment Petrol, 27(1): 3-26, doi: 10.1306/74D70646-2B21-11D7-8648000102C1865D.

Gao S, Collins M. 1992. Net sediment transport patterns inferred from grain-size trends, based upon definition of “transport vectors”. Sediment Geol, 81(1-2): 47-60, doi: 10.1016/0037-0738(92)90055-v.

Grebmeier J M, Cooper L W, Feder H M, et al. 2006. Ecosystem dynamics of the Pacific-influenced northern Bering and Chukchi seas in the Amerasian Arctic. Prog Oceanogr, 71(2): 331-361, doi: 10.1016/j.pocean.2006.10.001.

Grebmeier J M, Feder H M, McRoy C P. 1989. Pelagic-benthic coupling on the shelf of the northern Bering and Chukchi seas. II. Benthic community structure. Mar Ecol Prog Ser, 51: 253-268, doi: 10.3354/meps051253.

Honjo S, Krishfield R A, Eglinton T I, et al. 2010. Biological pump processes in the cryopelagic and hemipelagic Arctic Ocean: Canada Basin and Chukchi Rise. Prog Oceanogr, 85(3-4): 137-170, doi: 10.1016/j.pocean.2010.02.009.

Hwang J, Eglinton T I, Krishfield R A, et al. 2008. Lateral organic carbon supply to the deep Canada Basin. Geophys Res Lett, 35(11): L11607, doi: 10.1029/2008GL034271.

Jakobsson M, Mayer L, Coakley B, et al. 2012. The international bathymetric chart of the Arctic Ocean (IBCAO) version 3.0. Geophys Res Lett, 39(12): L12609, doi: 10.1029/2012GL052219.

Le Roux J P, Rojas E M. 2007. Sediment transport patterns determined from grain size parameters: Overview and state of the art. Sediment Geol, 202: 473-488, doi: 10.1016/j.sedgeo.2007.03.014.

McManus J. 1988. Grain size determination and interpretation//Tucker M. Techniques in sedimentology. Oxford, UK: Blackwell Scientific Publications, 63-85.

Merico A, Tyrrell T, Wilson P A. 2008. Eocene/Oligocene ocean de-acidification linked to Antarctic glaciation by sea-level fall. Nature, 452(7190): 979, doi: 10.1038/nature06853.

Middleton G V. 1976. Hydraulic interpretation of sand size distributions. J Geol, 84(4): 405-426, doi: 10.1086/628208.

Nagashima K, Asahara Y, Takeuchi F, et al. 2012. Contribution of detrital materials from the Yukon River to the continental shelf sediments of the Bering Sea based on the electron spin resonance signal intensity and crystallinity of quartz. Deep Sea Res Part II: Top Stud Oceanogr, 61-64: 145-154, doi: 10.1016/j.dsr2.2011.12.001.

Naidu A S, Creager J S, Mowatt T C. 1982. Clay mineral dispersal patterns in the north Bering and Chukchi seas. Mar Geol, 47(1-2): 1-15, doi: 10.1016/0025-3227(82)90016-0.

Nürnberg D, Wollenburg I, Dethleff D, et al. 1994. Sediments in Arctic sea ice: Implications for entrainment, transport and release. Mar Geol, 119: 185-214, doi: 10.1016/0025-3227(94)90181-3.

Nwaodua E C, Ortiz J D, Griffith E M. 2014. Diffuse spectral reflectance of surficial sediments indicates sedimentary environments on the shelves of the Bering Sea and western Arctic. Mar Geol, 355: 218-233, doi: 10.1016/j.margeo.2014.05.023.

O’Brien M C, MacDonald R W, Melling H, et al. 2006. Particle fluxes and geochemistry on the Canadian Beaufort Shelf: Implications for sediment transport and deposition. Cont Shelf Res, 26(1): 41-81, doi: 10.1016/j.csr.2005.09.007.

O’Brien M C, Melling H, Pedersen T F, et al. 2013. The role of eddies on particle flux in the Canada Basin of the Arctic Ocean. Deep Sea Res Part I: Oceanogr Res Pap, 71: 1-20, doi: 10.1016/j.dsr.2012.10.004.

Park C S, Hwang S, Yoon S O, et al. 2014a. Grain size partitioning in loess–paleosol sequence on the west Coast of South Korea using the Weibull function. Catena, 121: 307-320, doi: 10.1016/j.catena.2014.05.018.

Park Y H, Yamamoto M, Nam S I, et al. 2014b. Distribution, source and transportation of glycerol dialkyl glycerol tetraethers in surface sediments from the western Arctic Ocean and the northern Bering Sea. Mar Chem, 165: 10-24, doi: 10.1016/j.marchem.2014.07.001.

Poizot E, Méar Y. 2008. eCSedtrend: a new software to improve sediment trend analysis. Comput Geosci, 34(7): 827-837, doi: 10.1016/j.cageo.2007.05.022.

Poizot E, Méar Y, Biscara L. 2008. Sediment Trend Analysis through the variation of granulometric parameters: a review of theories and applications. Earth-Sci Rev, 86(1-4): 15-41, doi: 10.1016/j.earscirev.2007.07.004.

Polyak L, Alley R B, Andrews J T, et al. 2010. History of sea ice in the Arctic. Quat Sci Rev, 29(15-16): 1757-1778, doi: 10.1016/j.quascirev.2010.02.010.

Prins M A, Postma G, Weltje G J. 2000. Controls on terrigenous sediment supply to the Arabian Sea during the late Quaternary: the Makran continental slope. Mar Geol, 169(3-4): 351-371, doi: 10.1016/S0025-3227(00)00087-6.

Qin X G, Cai B G, Liu T. 2005. Loess record of the aerodynamic environment in the East Asia monsoon area since 60, 000 years before present. J Geophys Res: Solid Earth, 110(B1): B01204, doi: 10.1029/2004JB003131.

Reimnitz E, McCormick M, Bischof J, et al. 1998. Comparing sea-ice sediment load with Beaufort Sea shelf deposits: Is entrainment selective? J Sediment Res, 68(5): 777-787, doi: 10.2110/jsr.68.777.

Serreze M C, Crawford A D, Stroeve J C, et al. 2016. Variability, trends, and predictability of seasonal sea ice retreat and advance in the Chukchi Sea. J Geophys Res: Ocean, 121(10): 7308-7325, doi: 10.1002/2016JC011977.

Spielhagen R F, Baumann K H, Erlenkeuser H, et al. 2004. Arctic Ocean

deep-sea record of northern Eurasian ice sheet history. Quat Sci Rev, 23(11-13): 1455-1483, doi: 10.1016/j.quascirev.2003.12.015.

Stein R. 2008. Arctic Ocean sediments: Processes, proxies and paleoenvironment. Elsevier: Amsterdam, 35-84, doi: 10.1016/s1572-5480(08)00014-6.

Stickley C E, St John K, Koç N, et al. 2009. Evidence for middle Eocene Arctic sea ice from diatoms and ice-rafted debris. Nature, 460(7253): 376-384, doi: 10.1038/nature08163.

Sun D H, Bloemendal J, Rea D K, et al. 2002. Grain-size distribution function of polymodal sediments in hydraulic and aeolian environments, and numerical partitioning of the sedimentary components. Sediment Geol, 152(3-4): 263-277, doi: 10.1016/S0037-0738(02)00082-9.

Tucker III W B, Gow A J, Meese D A, et al. 1999. Physical characteristics of summer sea ice across the Arctic Ocean. J Geophys Res: Ocean, 104(C1): 1489-1504, doi: 10.1029/98JC02607.

VanLaningham S, Pisias N G, Duncan R A, et al. 2009. Glacial-interglacial sediment transport to the Meiji Drift, northwest Pacific Ocean: Evidence for timing of Beringian outwashing. Earth Planet Sci Lett, 277(1-2): 64-72, doi: 10.1016/j.epsl.2008.09.033.

Viscosi-Shirley C, Pisias N, Mammone K. 2003. Sediment source strength, transport pathways and accumulation patterns on the Siberian–Arctic's Chukchi and Laptev shelves. Cont Shelf Res, 23(11-13): 1201-1225, doi: 10.1016/S0278-4343(03)00090-6.

Wang W G, Dai S, Chen L L, et al. 2014. Magnetic susceptibility characteristics of surface sediments in Bering Sea and western Arctic Ocean: preliminary results. Acta Oceanologic Sinica, 36: 121-131, doi: 10.3969/j.issn.0253-4193.2014.09.014 (in Chinese with English abstract).

Watanabe E, Onodera J, Harada N, et al. 2014. Enhanced role of eddies in the Arctic marine biological pump. Nat Commun, 5(1): 3950, doi: 10.1038/ncomms4950.

Weingartner T, Aagaard K, Woodgate R, et al. 2005. Circulation on the north central Chukchi Sea shelf. Deep Sea Res Part II: Top Stud Oceanogr, 52(24-26): 3150-3174, doi: 10.1016/j.dsr2.2005.10.015.

Weingartner T J, Cavalieri D J, Aagaard K, et al. 1998. Circulation, dense water formation, and outflow on the northeast Chukchi Shelf. J Geophys Res: Ocean, 103(C4): 7647-7661, doi: 10.1029/98JC00374.

Weltje G J, Prins M A. 2003. Muddled or mixed? Inferring palaeoclimate from size distributions of deep-sea clastics. Sediment Geol, 162(1-2): 39-62, doi: 10.1016/s0037-0738(03)00235-5.

Weltje G J, Prins M A. 2007. Genetically meaningful decomposition of grain-size distributions. Sediment Geol, 202(3): 409-424, doi: 10.1016/j.sedgeo.2007.03.007.

Woodgate R A, Stafford K M, Prahl F G. 2015. A synthesis of year-round interdisciplinary mooring measurements in the Bering Strait (1990–2014) and the RUSALCA Years (2004–2011). Oceanography, 28(3): 46-67, doi: 10.5670/oceanog.2015.57.

Xiao J L, Chang Z G, Fan J W, et al. 2012. The link between grain-size components and depositional processes in a modern clastic lake. Sedimentology, 59(3): 1050-1062, doi: 10.1111/j.1365-3091.2011.01294.x.

Zhang T L, Wang R J, Polyak L, et al. 2019. Enhanced deposition of coal fragments at the Chukchi margin, western Arctic Ocean: Implications for deglacial drainage history from the Laurentide Ice Sheet. Quat Sci Rev, 218: 281-292, doi: 10.1016/j.quascirev.2019.06.029.

Zhou X, Yang W Q, Xiang R, et al. 2014. Re-examining the potential of using sensitive grain size of coastal muddy sediments as proxy of winter monsoon strength. Quat Int, 333: 173-178, doi: 10.1016/j.quaint.2013.12.013.